*33rd EPS Conference on Plasma Phys. Rome, 19 - 23 June 2006 ECA Vol.**30I**, P-2.158 (2006)*

# Turbulence simulations of a full poloidal cross section compared to Reynolds stress and zonal flows measured in the edge of TEXTOR.

M. Vergote, M. Van Schoor, Y. Xu, S. Jachmich

*Euratom-Etat Belge' - Associatie 'Euratom-Belgische Staat', Ecole Royale Militaire - Koninklijke Militaire School, Avenue de la Renaissance, Renaissancelaan 30, B-1000 Brussels, Belgium , Partner in the Trilateral Euregio Cluster (TEC).*

## Introduction

It is well known that understanding the nature of plasma turbulence in a tokamak is critical for the successful pursuit of fusion based energy production. In this paper we discuss the modelling of turbulence and the interaction between the turbulence and the background flows by means of a pseudo spectral simulation code and compare these simulations to experimental data recently obtained in TEXTOR using a new Reynolds stress probe. With this probe, mounted on a fast manipulator, we measure floating potential and density fluctuations at different radial positions in the edge of the tokamak. The pseudo spectral code is based on the 2D Hasegawa-Wakatani (HW) model [1], completed with magnetic inhomogeneity terms introducing curvature effects and implements correctly all the different operators in toroidal geometry with circular cross section. The local version of this code was already used with succes in the past to simulate ohmic shots on CASTOR and TEXTOR [2, 3]. We study the temporal behavior of the anomalous particle losses and the Reynolds stresses and correlate these to the presence of zonal flows. The relative importance of the different terms in the equations is discussed as well.

## Theoretical modelling

The local simulations of CASTOR data already showed a rather strong influence of the magnetic inhomogeneity terms and of the correct normalization on the poloidal distribution of the fluctuations [2]. In order to get a rough idea how the large scales behave (which are impossible to generate in the local version), we continued our study by extending the simulated domain onto a complete poloidal annulus. We recalculate the HW-equations by taking - in a torus with circular cross section and without Grad-Shafranov shift - the curl of the total momentum equation and projecting upon $\vec{u}_{\|} \approx \vec{u}_{\varphi}$: as a first approximation, we implement the HW equations in the 2D poloidal plane, considering a magnetic field in the $\vec{u}_{\varphi}$-direction, with strength $B_0 R_0/R$. With the proper non-dimensional definition of the electron density $n' = \frac{n}{n_0}\frac{L_n}{\rho_s}$ and the potential $\phi' = \frac{e\phi}{k_B T}\frac{L_n}{\rho_s}$, we can write our model equations for the vorticity $\frac{R}{R_0}\nabla'^2_{\perp}\phi'$ (toroidal expression) and the fluctuating electron density :

$$(\partial_{t'}+\frac{R}{R_0}[\phi',\ ])\left(\frac{R}{R_0}\nabla_\perp'^2\phi'\right) = \frac{C_1}{(R/R_0)}(\phi'-n')-\frac{1}{(R/R_0)}\mathbf{K}'(n')+\frac{1}{2}\left(\frac{R}{R_0}\nabla_\perp'^2\phi'\right)\mathbf{K}'(\phi') + C_2\nabla_\perp'^2\left(\frac{R}{R_0}\nabla_\perp'^2\phi'\right)-\nu^*\left(\frac{R}{R_0}\nabla_\perp'^2\phi'\right) \quad (1)$$

$$(\partial_{t'}+\frac{R}{R_0}[\phi',\ ])n' = C_1(\phi'-n')+\frac{R}{R_0}\frac{1}{r'}\partial_\theta\phi'+\mathbf{K}'(\phi'-n')+C_2\nabla_\perp'^2 n' \quad (2)$$

Here the primes denote dimensionless quantities ($r'=r/\rho_s$, $t'=\omega_{ci}\frac{\rho_s}{L_n}t$, with $\rho_s$ the ion Larmor radius at electron temperature, $\omega_{ci}$ the ion cyclotron frequency and $L_n/\rho_s=|\partial_{r'}\ln n_o(r)|^{-1}$ the normalized background density gradient scale length) and $[A,B]=\frac{1}{r'}(\partial_{r'}A\partial_\theta B-\partial_\theta A\partial_{r'}B)$. The parallel coupling coefficient (electron conductivity) is abbreviated by $C_1=\frac{kT_e\sigma_\parallel}{e^2\omega_{ci}n_o}\frac{L_n}{\rho_s}k_\parallel^2$ and is taken constant in our 2D-approach. This also means that we do not consider magnetic shear effects. The numerical value used for $C_1(0.3)$ corresponds to $k_\parallel=1/qR_0$. The friction due to neutrals $\nu^*=n_{neutrals}<\sigma.\mathrm{v}>/(\omega_{ci}\rho_s/L_n)$ [4] (with $n_{neutrals}=0.01\,n_0$), the kinematic ion shear viscosity $C_2=2.5\frac{\mu}{\omega_{ci}\rho_s^2}\frac{L_n}{\rho_s}$ and the particle diffusion provide numerical stability. The curvature operator $\mathbf{K}'(f)=2\frac{L_n}{\rho_s}[\frac{R}{R_0},f]=\omega_B(\frac{\cos\theta}{r'}\partial_\theta+\sin\theta\partial_{r'})f$, with $\omega_B=\frac{2L_n}{R_0}$. Note that this terms couples neighboring poloidal modes(m), as does the nonlinearity $[\phi,\bullet]$ between so-called triads.

**Simulations and comparison with the experiment**

The coefficients $C_2$ and $\omega_B$ are computed according to the edge parameters of TEXTOR (Deuterium plasma at $T_0\approx 40$eV, reference density $n_0=0.5\times10^{19}\mathrm{m}^{-3}$, $\nabla n_o=-10^{20}\mathrm{m}^{-4}$ and $R_0=1.75m$, $a=0.48m$, $B_T=1.5T$). The evolution of the dynamical equations is computed by a pseudospectral code on an annulus between $r_{min}=0.40$m and $r_{max}=0.48$m, on a computational grid of $16\times256$ nodes in $(r,\theta)$. The domain is covered radially by Gauss-Lobatto points, as prescribed by the spectral method based on differentiation matrices [5]. The real space between two grid points in the center of the domain ($\approx 8$ mm) is based on the discretization unit $\rho_0=50\rho_s$. The driving background density $n_o(r)$ is assumed to remain unchanged. All primed densities have in that respect poloidally always a zero mean and the background density is left out of the curvature terms. Poloidally we apply periodic boundary conditions, while radially the potential is fixed at the outer radius $\phi|_{r_{max}}=0$ , but is free to evolve inwards as is the case in the real experiment ($\partial_r\phi_{m=0}|_{r_{min}}=0$ and $\phi_{m\neq0}|_{r_{min}}=0$ ). Poloidal mode numbers in absolute value above $m=85$ are discarded according the 2/3's rule, those above $m=64$ are artificially damped by a hyperviscosity and the time stepping algorithm is based on the Karniadakis SS3-scheme. We have performed different runs to study the importance of the different terms in the equations. The reference run is the one in which all terms in Eqs. (1) and (2) are included, and is called the toroidal model(TOR). A second run is performed by leaving out the nonlinear

correction term (third term on rhs. of Eq. (1)) and by putting $R = R_0$, reducing the model to the commonly used cylindrical one (CYL), with curvature terms coming solely from the magnetic inhomogeneity making the $\vec{E} \times \vec{B}$ and diamagnetic velocities non-divergence free. In a third run all curvature effects are removed, representing a pure drift wave turbulence (DW). All runs have the same initial conditions and show a similar transient linear growth until the nonlinear saturated regime is established (see Fig. 1 - upper panel). The TOR simulation shows the strongest turbulent 'metastable' phase (at $t' \approx 100$ - lower panel) before relaxing to the rather stationary turbulent phase afterwards. Note that in the stationary phase the absolute values of both the Reynolds stress ($\approx 10^6 \mathrm{m}^2/\mathrm{s}^2$) and $D$ ($= \Gamma/\nabla n_o \approx 0.8 \mathrm{m}^2/\mathrm{s}$) correspond rather well with the experimental values at the edge during ohmical discharges in TEXTOR [6]. Having a closer look at the two equations in the TOR model, we define the transfert spectra as the mean contribution to the total change in energy of each driving/coupling term per timestep. We find that the turbulence is dominated by the background density driving term $\frac{1}{r'}\partial_\theta \phi'$ in the smaller scales range ($m > 4$, see Fig. 2(a)), and that the curvature terms only have a minor influence (Fig. 2(c)) with respect to the parallel coupling (Fig. 2(b)), except for $m = 0$.

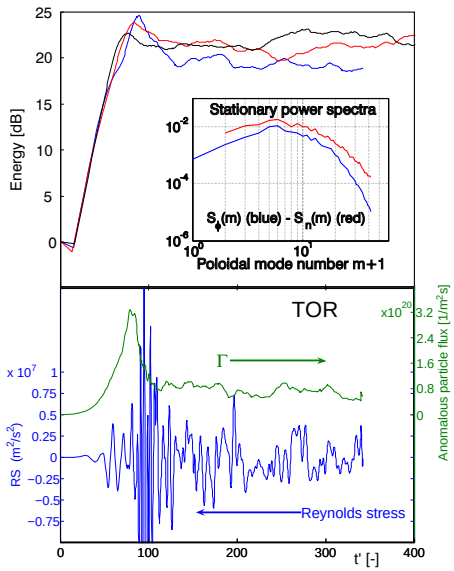


*Figure 1: up: fluctuation energy for runs TOR (blue), CYL (red) and DW (black); insert: stationary power spectra for potential(blue) and density(red) ; down: time trace of the Reynolds stress(RS, blue) and particle flux (Γ, green) for the TOR run.*

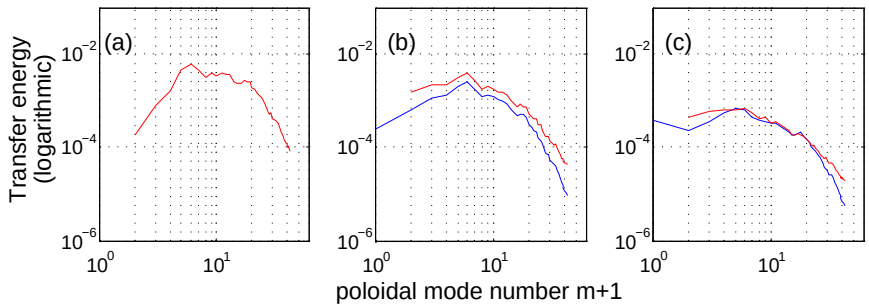


*Figure 2: Energy transfer spectra in stationary turbulence (TOR): (a) for the linear driving term $\frac{1}{r'}\partial_\theta \phi'$ in the density equation; (b) for the parallel ($C_1$) term in the vorticity (blue) and density (red) equation; (c) for the linear curvature ($\omega_B$) terms in the vorticity (blue) and density (red) equation.*

We can corroborate this statement by looking at the cross-phase between the density and the potential, which turns out to be $\approx 0.4$ (closer to zero than it is to $\pi/2$, as would be the case in interchange turbulence). The cross-correlation coefficient ($\approx 0.8$ calculated) on the other hand confirms the value found in local simulations with comparable parameters (see Ref. [3] for $C_1$

constant). The comparison with the real experiment shows (see Fig. 3) a common feature: the existence of large scale zonal flows(ZF). The lowest frequency ZF ($c_s/2\pi R_0$ is of order 10 kHz) and their harmonics are dominantly present in the raw floating potential data in TEXTOR [3]. The time traces from the TOR/CYL simulations (once in saturation, blue curve), show these large dominant structures as well. By looking at the time-trace of the power in the different mode numbers (not shown here), we can shed light on how these large structures are being formed. First, the linearly most unstable ($k'_\theta \approx 1$ or $m \approx 15$) modes grow fastest. It is only after a while that larger (linearly more stable) modes acquire more energy. As at that same moment the earliest modes lose in average energy, it is probably through the nonlinearity $[\phi, \bullet]$ that this process takes place: the Reynolds stress (in the vorticity equation).

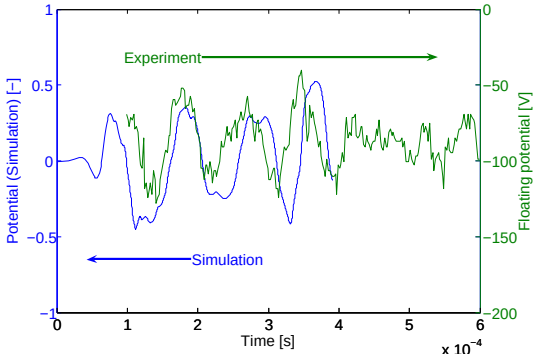


*Figure 3: Potential in simulation TOR (blue) and raw floating potential in TEXTOR (green).*

**Conclusion**

We have implemented a simple drift wave turbulence model simulating the edge of TEXTOR in presence of neutrals, with different assumptions on the curvature(TOR, CYL, DW). We discussed the different contributions in the equations for the TOR case. Although this 2D turbulence model is much simplified, some similarities are striking (values of $\Gamma$, RS and the ZF structures) and so we are planning to proceed these simulations to further analyse their outcome and to extend their applicability.

**References**

[1] Hasegawa and Wakatani. *Physics of Fluids*, 27:611, 1984.

[2] M. Vergote et al. *Plasma Physics and Controlled Fusion*, 48:S75, 2006.

[3] M. Vergote et al. Proceedings of the 17th International Conference on Plasma-Surface Interactions, Hefei, China (May, 22-26, 2006).

[4] M. Harrison. *Physics of plasma-wall interactions in controlled fusion*, volume NATO ASI of *Series B 131*. New York, Plenum Press, 1986.

[5] J. Weideman and S. Reddy. *ACM transactions on mathematical software*, 26(4):465, 2000.

[6] Y. Xu et al. *Phys. Rev. Letters*, 2006. submitted to Phys. Rev. Letters.